Randomly coupled Ising models

S. Galam
Groupe de Physique des Solides, Tour 23, 2 place Jussieu, 75251 Paris, Cedex 05, France

S. R. Salinas
Instituto de Fisica, Universidade de São Paulo, Caixa Postal 20516, 01452-990, São Paulo, Brazil

Y. Shapir
Department of Physics and Astronomy, University of Rochester, Rochester, New York 14627-0011
(Received 25 April 1994; revised manuscript received 19 September 1994)

We consider the phase diagram of two randomly coupled Ising models to mimic the successive phase transitions in plastic crystals. Detailed mean-field calculations are performed. Depending on the strength of the couplings, the phase diagrams display three ordered phases and some multicritical points. A tetracritical point is found to turn bicritical as the strength of the couplings increases. The nature of this multicritical point is then analyzed by means of a momentum-space renormalization-group calculation. Using the replica trick, we obtain an effective n-component spin Hamiltonian. The random coupling is found to be relevant and shown to have drastic effects on the multicritical behavior. The lower critical dimension is estimated to be $d_l=2$. In the $n=0$ limit, to first order in the parameter $\epsilon=4-d$, a system of seven recursion relations is obtained. Although there is a stable fixed point, it cannot be reached from physically acceptable initial conditions. We give arguments to support a runaway of the flow lines associated with a fluctuation-induced first-order transition.

I. INTRODUCTION

Coupled spin models have been used to account for the interplay of translational and rotational degrees of freedom in plastic crystals. Lowering the temperature from the liquid phase, plastic crystals undergo a first-order transition to an intermediate thermodynamically stable plastic phase, where rotational disorder coexists with a translationally ordered state. At lower temperatures, there is another phase transition, usually of first order, to the solid phase. Due to steric hindrances, the coupling between translational and rotational degrees of freedom is expected to play a fundamental role in the onset of these transitions.

Bilinear couplings between effective spin variables, which are supposed to mimic translational and rotational degrees of freedom, have been used to explain the thermodynamic behavior in the plastic phase.[1] In fact, there are earlier mean-field studies of a lattice-gas model for the melting transition with the inclusion of extra spin variables to represent the rotational degrees of freedom.[2] More recently, tetralinear translational-rotational couplings have also been considered,[3] and shown to be generated by a special kind of compressible model.[4] However, the dynamics of reorientations in the plastic phase is rather complex. Besides the librations around the preferred orientations allowed by symmetry, there are also large amplitude jumps from one orientation to another. The long reorientation times give room to a relaxation of the translational degrees of freedom. This process suggests the existence of an "excited molecular state" surrounded by a local deformation of the lattice, which should be equivalent to the presence of a virtual impurity. Random fields have been invoked to take into account this mechanism.[5] According to these arguments, Galam has introduced a system of two Ising models, with uniform bilinear couplings, in the present of a random field affecting one of the Ising variables. However, from the requirements of symmetry, it should be more appropriate to consider an alternative model with random strengths of the rotational-translational bilinear couplings. On this basis, we perform an analysis of two distinct Ising ferromagnetic systems in the presence of random bilinear couplings.

The model studied in this paper is given by the effective spin Hamiltonian

$$H=-J_1\sum_{(ij)}S_iS_j-J_2\sum_{(ij)}T_iT_j-\sum_{i=1}^{N}\eta_iS_iT_i\ , \tag{1}$$

where the Ising spin variables $S_i=\pm 1$ mimic the rotational degrees of freedom, the extra spin variables $T_i=\pm 1$ mimic the translational degrees of freedom, and (ij) labels a pair of nearest-neighbor sites on a hypercubic lattice of N sites and dimension d. The independent, identically distributed random variables, $\{\eta_i\}$, are associated with an even probability distribution, $p(\eta_i)$, which does not destroy the symmetry of the ordered phases. We always assume $J_1>0$, and $J_2>0$, with a ferromagnetic ground state.

During the last decade, a considerable effort has been devoted to the analysis of the phase transitions in random and disordered systems. The interplay between theory and experiment has been very fruitful. For example, the previous theoretical investigations of a simple ferromagnetic Ising model in a random field have been shown to be relevant to account for the behavior of disordered antiferromagnetic crystals in a uniform field. The study of disordered spin systems still presents some challenging theoretical problems. Although we were in part motivated by the associations with the behavior of plastic crystals, we have introduced a coupled spin Hamiltonian that is simple enough to be amenable to some calculations which provide an instrumental step towards the understanding of more realistic models. In the present case of random bilinear couplings, we were able to perform detailed mean-field calculations, as well as a rather complete renormalization-group analysis, to display a number of distinct phases and multicritical points.

In Sec. II, we present an exact solution of a long-range version of the model Hamiltonian. As the problem is self-averaging, this mean-field solution can be obtained without using the replica trick. In Sec. III, we calculate the main features of the $T-p$ phase diagram, where T is the temperature and $p=J_2/J_1$, for a double-δ distribution. For weak bilinear couplings, in addition to the simple ordered phases, (i) $m_1=\langle S\rangle\neq 0$ and $m_2=\langle T\rangle=0$, and (ii) $m_1=0$, and $m_2\neq 0$, there is also a mixed phase, (iii) $m_1\neq 0$ and $m_2\neq 0$. For strong bilinear couplings, this mixed phase is no longer present. We have performed some analytical and numerical calculations to locate the phase boundaries and the multicritical points. This is probably one of the simplest models to display a tetracritical point which turns into bicritical as a function of a parameter. On the basis of the fully understood mean-field phase diagrams, we have performed a renormalization-group calculation to analyze the multicritical behavior. Along the lines of previous work,[6,7] for random-anisotropy spin models, we use the replica trick to write an effective n-component Hamiltonian in momentum space. In Sec. IV, we obtain a set of seven recursion relations up to terms of order $\epsilon=4-d$. In the $n=0$ limit, we have a rich structure of fixed points and make contact with the results of an analysis of the multicritical behavior in the context of a system of six recursion relations for a magnetic model with random competing anisotropies.[8] We give some arguments to show that the stable fixed points cannot be reached from physically acceptable initial conditions. As in previous calculations for spin models with random anisotropies,[6,7] this seems to indicate the possibility of occurrence of a fluctuation-induced first-order transition. In Sec. V, we obtain the crossover exponent, $\Phi=(\epsilon-4\eta)\nu$, from the behavior of the decoupled Ising models. The random couplings are then relevant in two and three dimensions. The lower critical dimension is found to be $d_l=2$. Some conclusions are presented in Sec. VI.

II. MEAN-FIELD SOLUTION

The long-range, Curie-Weiss, version of the model Hamiltonian is given by

$$H=-\frac{J_1}{2N}\left[\sum_{i=1}^{N} S_i\right]^2-\frac{J_2}{2N}\left[\sum_{i=1}^{N} T_i\right]^2-\sum_{i=1}^{N}\eta_i S_i T_i \ , \qquad (2)$$

which yields the partition function

$$Z\{\eta_i\}=\mathrm{Tr}\exp\left\{\frac{\beta J_1}{2N}\left[\sum_i S_i\right]^2+\frac{\beta J_2}{2N}\left[\sum_i T_i\right]^2+\sum_i \beta\eta_i S_i R_i\right\} , \qquad (3)$$

where $\beta=(k_BT)^{-1}$, and the trace indicates a sum over spin configurations. Using the Gaussian identity

$$\int_{-\infty}^{+\infty}\exp(-x^2+2ax)dx=\sqrt{\pi}\exp(a^2) \ , \qquad (4)$$

we can write

$$Z\{\eta_i\}=\frac{1}{\pi}\int_{-\infty}^{+\infty}\int_{-\infty}^{+\infty}dx\,dy\,\exp(-x^2-y^2)\prod_{i=1}^{N}\mathrm{tr}\exp\left[\left[\frac{2\beta J_1}{N}\right]^{1/2}xS+\left[\frac{2\beta J_2}{N}\right]^{1/2}yT+\beta\eta_i ST\right] . \qquad (5)$$

Performing the trace over the spin variables and defining the new quantities

$$m_1=\left[\frac{2}{\beta J_1 N}\right]^{1/2}x \ , \qquad (6)$$

and

$$m_2=\left[\frac{2}{\beta J_2 N}\right]^{1/2}y \ , \qquad (7)$$

we have

$$Z\{\eta_i\}=\frac{\beta N}{2\pi}(J_1J_2)^{1/2}\int_{-\infty}^{+\infty}\int_{-\infty}^{+\infty}dm_1dm_2\exp\left\{-\frac{1}{2}N\beta J_1m_1^2-\frac{1}{2}N\beta J_2m_2^2+\sum_{i=1}^{N}\ln[2e^{\beta\eta_i}\cosh(\beta J_1m_1+\beta J_2m_2)+2e^{-\beta\eta_i}\cosh(\beta J_1m_1-\beta J_2m_2)]\right\} . \qquad (8)$$

In the thermodynamic limit, we can use the law of large numbers to write

$$Z=\frac{\beta N}{2\pi}(J_1J_2)^{1/2}\int_{-\infty}^{+\infty}\int_{-\infty}^{+\infty}dm_1dm_2\exp[-\beta N g(m_1,m_2)]\ , \tag{9}$$

where the free-energy functional, $g(m_1,m_2)$, is given by

$$g(m_1,m_2)=\tfrac{1}{2}J_1m_1^2+\tfrac{1}{2}J_2m_2^2-\frac{1}{\beta}E\{\ln[2e^{\beta\eta_i}\cosh(\beta J_1m_1+\beta J_2m_2)+2e^{-\beta\eta_i}\cos(\beta J_1m_1-\beta J_2m_2)]\}\ , \tag{10}$$

and $E\{\cdots\}$ indicates the expectation value with respect to the set of independent, identically distributed random variables, $\{\eta_i\}$. Given the temperature, the form of the distribution, and the parameters of the model, the thermodynamic solutions are determined by the minima of $g(m_1,m_2)$. In particular, the equations of state can be written in the form

$$m_1=E\left\{\frac{\tanh(\beta J_1m_1)+\tanh(\beta J_2m_2)\tanh(\beta\eta_i)}{1+\tanh(\beta J_1m_1)\tanh(\beta J_2m_2)\tanh(\beta\eta_i)}\right\}, \tag{11}$$

and

$$m_1=E\left\{\frac{\tanh(\beta J_2m_2)+\tanh(\beta J_1m_1)\tanh(\beta\eta_i)}{1+\tanh(\beta J_1m_1)\tanh(\beta J_2m_2)\tanh(\beta\eta_i)}\right\}. \tag{12}$$

For a symmetric probability distribution, with $E\{\eta_i^n\}=0$ for n odd, the critical lines are given by $t=1$ and $p=t$, where we have made use of the new dimensionless variables $t=(\beta J_1)^{-1}$ and $p=J_2/J_1$. To investigate the stability of these critical lines and the nature of the multicritical point at $t=p=1$, we can write the following expansion of the free-energy functional for a symmetric probability distribution:

$$\frac{1}{J_1}g(m_1,m_2)=-2t\ln 2-tE\{\ln\cosh(\beta\eta_i)\}+\frac{1}{2t}(t-1)m_1^2+\frac{p}{2t}(t-p)m_2^2+\frac{1}{12t^3}(m_1^4+p^4m_2^4)+\frac{p^2}{2t^3}E\{[\tanh(\beta\eta_i)]^2\}m_1^2m_2^2+\cdots\ . \tag{13}$$

III. PHASE DIAGRAMS FOR A DOUBLE-δ DISTRIBUTION

Let us consider a double-δ distribution given by

$$p(\eta_i)=\tfrac{1}{2}\delta(\eta_i-J_1\lambda)+\tfrac{1}{2}\delta(\eta_i+J_1\lambda)\ . \tag{14}$$

In this case the free-energy functional can be written as

$$\frac{1}{J_1}g(m_1,m_2)=-2t\ln 2-t\ln\cosh\left[\frac{\lambda}{t}\right]+\frac{1}{2}m_1^2+\frac{p}{2}m_2^2-t\ln\cosh\left[\frac{m_1}{t}\right]-t\ln\cosh\left[\frac{pm_2}{t}\right]-\frac{t}{2}\ln\left[1-\tanh^2\left[\frac{\lambda}{t}\right]\tanh^2\left[\frac{m_1}{t}\right]\tanh^2\left[\frac{pm_2}{t}\right]\right]\ , \tag{15}$$

from which we obtain the expansion

$$\frac{1}{J_1}g(m_1,m_2)=-2t\ln 2-t\ln\cosh\left[\frac{\lambda}{t}\right]+\frac{1}{2t}(t-1)m_1^2+\frac{p}{2t}(t-p)m_2^2+\frac{1}{12t^3}\left[m_1^4+p^4m_2^4+6p^2\tanh^2\left[\frac{\lambda}{t}\right]m_1^2m_2^2\right]+\cdots\ . \tag{16}$$

As mentioned in the previous section, the paramagnetic critical lines are given by $t=1$ and $p=t$. From an analysis of the quartic terms, it follows that there is a tetracritical point at $t=p=1$, for $\lambda<\lambda_0=\tanh^{-1}(1/\sqrt{3})=0.658\,47\ldots$, which becomes bicritical for $\lambda>\lambda_0$. In Figs. 1–3, we show some typical phase diagrams for $0<\lambda<\lambda_0$. In Fig. 4, for $\lambda>\lambda_0$, we indicate that the mixed phase, $m_1\neq 0$ and $m_2\neq 0$, collapses into a first-order boundary. For $t<1$, the upper critical line in Figs. 1–3 is given by

$$\left[m_2\tanh\left[\frac{\lambda}{t}\right]\right]^2+t=1\ , \tag{17}$$

with $m_2=\tanh(pm_2/t)$. The lower critical line is given by

$$p\left[m_1\tanh\left[\frac{\lambda}{t}\right]\right]^2+t=p\ , \tag{18}$$

with $m_1=\tanh(m_1/t)$. Analytical expressions for these

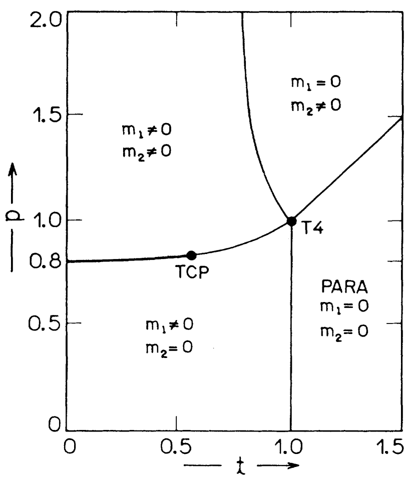

FIG. 1. Typical mean-free phase diagram for $0<\lambda<0.447\,74\ldots$ (this figure was drawn for $\lambda=0.4$). The light solid lines represent second-order phase transitions. The heavy line is a first-order transition. We indicate a tetracritical (T4) and a tricritical (TCP) point.

lines can be written in the immediate vicinity of the tetracritical point. Also, it is not difficult to locate the tricritical points.

From Eq. (15), we obtain some analytical results for the phase diagram at $T=0$. In the $\lambda-p$ space there are three possibilities: (i) $m_1=1$, and $m_2=1$, with $g/J_1=-1/2-p/2$, for $\lambda<1$ and $\lambda<p$; (ii) $m_1=1$, and $m_2=0$, with $g/J_1=-\frac{1}{2}-\lambda$, for $\lambda>0$; and (iii) $m_1=0$, and $m_2=1$, with $g/J_1=-p/2-\lambda$, for $\lambda>0$. So we can draw the phase diagram of Fig. 5, where the solid lines indicate first-order transitions. An asymptotic calculation near $t=0$ and $p=1$, for $\frac{1}{2}<\lambda<\lambda_0$, shows that there

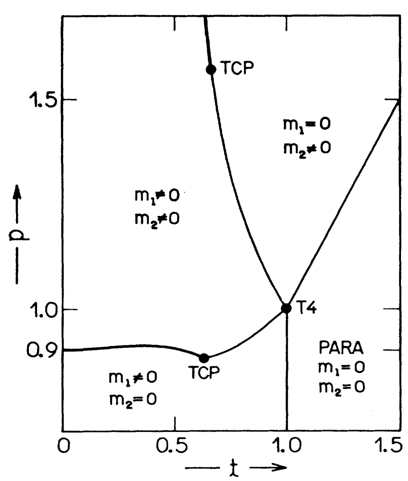

FIG. 2. Typical mean-field diagram for $0.447\,74\ldots<\lambda<\frac{1}{2}$. Besides the tetracritical point, there are also two tricritical points. The heavy solid lines indicate first-order transitions. This figure was drawn for $\lambda=0.45$.

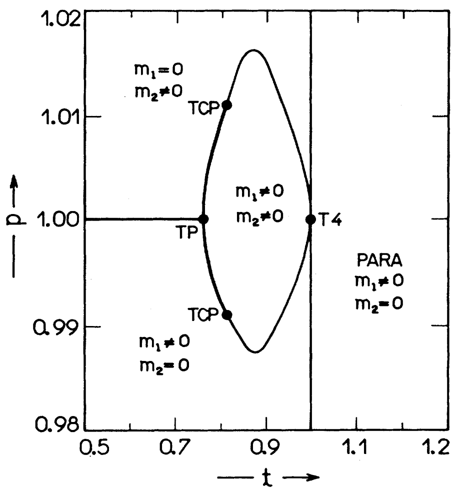

FIG. 3. Typical mean-field phase diagram for $\frac{1}{2}<\lambda<0.658\,47\ldots$ (this figure was drawn for $\lambda=0.58$). The mixed phase is restricted to a small internal region of the phase diagram. The heavy lines indicate first-order transitions. TP is a triple point.

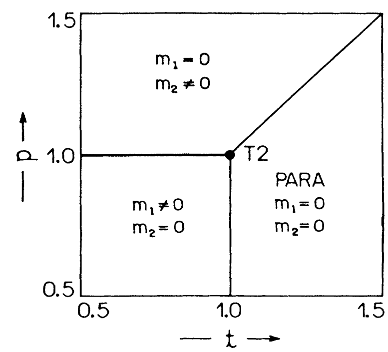

FIG. 4. Typical mean-field phase diagram for $\lambda>0.658\,47\ldots$. The first-order boundary between the ordered phases ends at a bicritical point (T2). The mixed phase is no longer present.

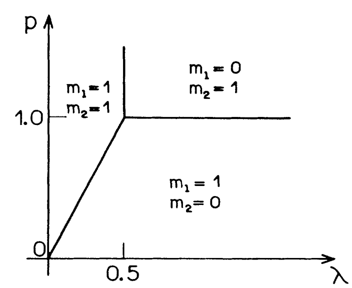

FIG. 5. Phase diagram at the ground state ($t=0$). The solid lines represent first-order transitions.

is no mixed phase, with $m_1 \neq 0$ and $m_2 \neq 0$, in this region of the phase diagram.

The typical phase diagrams sketched in Figs. 1–4 can be drawn on the basis of the analytical results near the multicritical point and in the vicinity of the ground state. In Fig. 1, we show a typical phase diagram for $0<\lambda<0.44774\ldots$. The upper boundary of the mixed phase is always of second order. The lower boundary, however, turns into first order at a tricritical point. In the narrow region $0.44774\ldots<\lambda<\frac{1}{2}$, as indicated in Fig. 2, besides the tetracritical point, there are two tricritical points along the boundary of the mixed phase. In Fig. 3, for $\frac{1}{2}<\lambda<0.68547\ldots$, there is also a triple point, as the mixed phase no longer exists at low temperatures. Finally, for $\lambda>\lambda_0$, there is a first-order line at $p=1$, from $t=0$ to the bicritical point at $t=1$. We have performed numerical calculations to check the location of the transition lines and the multicritical points.

It is interesting to look at the phase diagram on the $t-\lambda$ plane, for $p=1$, which corresponds to the symmetric form of the model. As shown in Fig. 6, this phase diagram displays a multicritical point at $t=1$ and $\lambda=\lambda_0=0.65847\ldots$, and a first-order transition line between the ordered phases. Due to the symmetry of the model Hamiltonian, the phases $m_1\neq 0$; $m_2=0$ and $m_1=0$; $m_2\neq 0$ are completely equivalent. In agreement with the graphs of Fig. 3, for $\frac{1}{2}<\lambda<\lambda_0$, as the temperature is raised we cross a first-order boundary to enter into an ordered region with $m_1=m_2\neq 0$.

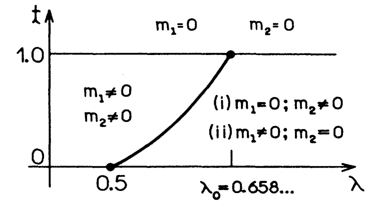

FIG. 6. Mean-field phase diagram for the symmetric case ($p=1$). The heavy line represents a first-order transition.

IV. RENORMALIZATION-GROUP CALCULATIONS

The partition function associated with the model Hamiltonian 1 is given by the expression

$$Z\{\eta_i\}=\mathrm{Tr}\exp\left[\beta J_1\sum_{(ij)}S_iS_j+\beta J_2\sum_{(ij)}T_iT_j+\sum_{i=1}^{N}\beta\eta_iS_iT_i\right]. \tag{19}$$

We can use the generalized Gaussian identity,[9]

$$\exp\left[\sum_{(ij)}K_{ij}S_iS_j\right]=\frac{1}{A}\left[\prod_{i=1}^{N}\int_{-\infty}^{+\infty}d\sigma_i\right]\exp\left[-\frac{1}{2}\sum_{i,j}(K^{-1})_{ij}\sigma_i\sigma_j+\sum_{i=1}^{N}\sigma_iS_i\right], \tag{20}$$

where $A=\sqrt{\pi^N D}$, and D is the determinant of the matrix K, to write Eq. (19) in the form

$$Z\{\eta_i\}=\frac{1}{B}\mathrm{Tr}\left[\prod_{i=1}^{N}\int_{-\infty}^{+\infty}d\sigma_i\int_{-\infty}^{+\infty}d\tau_i\right]\exp\left\{-\frac{1}{2}\sum_{i,j}(K_1^{-1})_{ij}\sigma_i\sigma_j-\frac{1}{2}\sum_{i,j}(K_2^{-1})_{ij}\tau_i\tau_j+\sum_{i=1}^{N}(\sigma_iS_i+\tau_iT_i+\beta\eta_iS_iT_i)\right\}, \tag{21}$$

where $B=\pi^N\sqrt{D_1D_2}$. Performing the trace over the discrete spin variables, we have

$$Z\{\eta_i\}=\frac{1}{B}\left[\prod_{i=1}^{N}\int_{-\infty}^{+\infty}d\sigma_i\int_{-\infty}^{+\infty}d\tau_i\right]\exp\left\{-\frac{1}{2}\sum_{i,j}(K_1^{-1})_{ij}\sigma_i\sigma_j-\frac{1}{2}\sum_{i,j}(K_2^{-1})_{ij}\tau_i\tau_j\right\}\times\prod_{i=1}^{N}2[e^{\beta\eta_i}\cosh(\sigma_i+\tau_i)+e^{-\beta\eta_i}\cosh(\sigma_i-\tau_i)]. \tag{22}$$

Now we introduce n replicas of the model and perform an average over the $\{\eta_i\}$ configurations to obtain the expression

$$\langle(Z\{\eta_i\})^n\rangle=\frac{1}{B^n}\left[\prod_{i=1}^{N}\prod_{\alpha=1}^{n}\int_{-\infty}^{+\infty}d\sigma_i^\alpha\int_{-\infty}^{+\infty}d\tau_i^\alpha\right]\exp\left\{-\frac{1}{2}\sum_\alpha\sum_{i,j}(K_1^{-1})_{ij}\sigma_i^\alpha\sigma_j^\alpha-\sum_\alpha\sum_{i,j}(K_2^{-1})_{ij}\tau_i^\alpha\tau_j^\alpha\right\}\times\prod_{i=1}^{N}\left\langle\prod_{\alpha=1}^{N}2[e^{\beta\eta_i}\cosh(\sigma_i^\alpha+\tau_i^\alpha)+e^{-\beta\eta_i}\cosh(\sigma_i^\alpha-\tau_i^\alpha)]\right\rangle, \tag{23}$$

where the averages should be taken with respect to the double-δ probability distribution given by Eq. (14). After a straightforward expansion about the paramagnetic saddle point, we have

$$\langle(Z\{\eta_i\})^2\rangle=\frac{C}{B^n}\left[\prod_{i=1}^{N}\prod_{\alpha=1}^{N}\int_{-\infty}^{+\infty}d\sigma_i^\alpha\int_{-\infty}^{+\infty}d\tau_i^\alpha\right]\exp\left\{-\frac{1}{2}\sum_\alpha\sum_{i,j}(K_1^{-1})_{ij}\sigma_i^\alpha\sigma_j^\alpha-\frac{1}{2}\sum_\alpha\sum_{i,j}(K_2^{-1})_{ij}\tau_i^\alpha\tau_j^\alpha+\sum_{i=1}^{N}\sum_{\alpha=1}^{n}W_i+\frac{1}{2}(\tanh\beta\eta)^2\sum_{i=1}^{N}\left[\sum_{\alpha=1}^{n}\sigma_i^\alpha\tau_i^\alpha\right]^2\right\}, \tag{24}$$

where

$$W_i=\frac{1}{2}(\sigma_i^\alpha)^2+\tfrac{1}{2}(\tau_i^\alpha)^2-\tfrac{1}{12}(\sigma_i^\alpha)^4-\tfrac{1}{12}(\tau_i^\alpha)^4-(\tanh\beta\lambda)^2(\sigma_i^\alpha)^2(\tau_i^\alpha)^2 , \quad (25)$$

the prefactor C depends on λ, and we have kept terms up to fourth order in the spin fields. Thus we can write the effective Hamiltonian

$$H_{\text{eff}}=H_0+H_p , \quad (26)$$

where

$$H_0=-\frac{1}{2}\sum_{\alpha=1}^{N}\sum_{i,j}(K_1^{-1}-\delta_{ij})_{ij}\sigma_i^\alpha\sigma_j^\alpha-\frac{1}{2}\sum_{\alpha=1}^{N}\sum_{i,j}(K_2^{-1}-\delta_{ij})_{ij}\tau_i^\alpha\tau_j^\alpha , \quad (27)$$

and

$$H_p=-\sum_{i=1}^{N}\sum_{\alpha=1}^{n}[\tilde{u}_1(\sigma_i^\alpha)^4+\tilde{u}_2(\tau_i^\alpha)^4+\tilde{w}(\sigma_i^\alpha)^2(\tau_i^\alpha)^2]+\tilde{v}\sum_{i=1}^{N}\left[\sum_{\alpha=1}^{n}\sigma_i^\alpha\tau_i^\alpha\right]^2 , \quad (28)$$

where

$$\tilde{u}_1=\tilde{u}_2=\tfrac{1}{12} , \quad (29)$$

$$\tilde{w}=(\tanh\beta\lambda)^2 , \quad (30)$$

and

$$\tilde{v}=\tfrac{1}{2}(\tanh\beta\lambda)^2 . \quad (31)$$

It should be noted that we can also use a Gaussian probability distribution for the set of random variables $\{\eta_i\}$ to obtain a similar effective Hamiltonian.

Now we introduce the Fourier representation,

$$\sigma_l=\frac{1}{N}\sum_{\mathbf{q}}\hat{\sigma}_{\mathbf{q}}e^{i\mathbf{q}\cdot\mathbf{l}} , \quad (32)$$

where l is a vector of a hypercubic d-dimensional lattice, and the sum is over the first Brillouin zone. After performing a low-momentum expansion and rescaling the spin fields, we have

$$H_0=-\frac{1}{2}\int_q\sum_\alpha(r_1+q^2+\cdots)\sigma_q^\alpha\sigma_{-q}^\alpha-\frac{1}{2}\int_q\sum_\alpha(r_2+q^2+\cdots)\tau_q^\alpha\tau_{-q}^\alpha , \quad (33)$$

and

$$H_p=\sum_\alpha\int_{q_1}\int_{q_2}\int_{q_3}(-u_1\sigma_{q_1}^\alpha\sigma_{q_2}^\alpha\sigma_{q_3}^\alpha\sigma_{-q_1-q_2-q_3}^\alpha-u_2\tau_{q_1}^\alpha\tau_{q_2}^\alpha\tau_{q_3}^\alpha\tau_{-q_1-q_2-q_3}^\alpha-w\sigma_{q_1}^\alpha\sigma_{q_2}^\alpha\tau_{q_3}^\alpha\tau_{-q_1-q_2-q_3}^\alpha)+v\sum_{\alpha,\beta}\int_{q_1}\int_{q_2}\int_{q_3}\sigma_{q_1}^\alpha\tau_{q_2}^\alpha\sigma_{q_3}^\beta\tau_{-q_1-q_2-q_3}^\beta , \quad (34)$$

where the vector arrows and the hats have been dropped to simplify the notation, and the coefficients are given by

$$r_1=\frac{1}{a^2\beta J_1}(1-2d\beta J_1) , \quad (35)$$

$$r_2=\frac{1}{a^2\beta J_2}(1-2\beta J_2) , \quad (36)$$

$$(u_1,u_2)\left[\frac{4\beta d^2}{a^2}\right](J_1^2\tilde{u}_1,J_2^2\tilde{u}_2) , \quad (37)$$

$$(w,v)=\left[\frac{4\beta d^2}{a^2}\right]^2J_1J_2(\tilde{w},\tilde{v}) , \quad (38)$$

where a is the lattice parameter of the d-dimensional hypercubic lattice. Although there are only four types of quartic terms in Eq. (34), it is easy to see that additional quartic terms which are associated with the full symmetry of the Hamiltonian in the n-vector space, will be generated at the first stage of the normalization-group perturbation scheme. We thus work with the more general perturbation,

$$H_p=\sum_{\alpha,\beta}\int_{q_1}\int_{q_2}\int_{q_3}\{-(u_1+v_1\delta_{\alpha\beta})\sigma_{q_1}^\alpha\sigma_{q_2}^\alpha\sigma_{q_3}^\beta\sigma_{-q_1-q_2-q_3}^\beta-(u_2+v_2\delta_{\alpha\beta})\tau_{q_1}^\alpha\tau_{q_2}^\alpha\tau_{q_3}^\beta\tau_{-q_1-q_2-q_3}^\beta-(w+\hat{w}\delta_{\alpha\beta})\sigma_{q_1}^\alpha\sigma_{q_2}^\alpha\tau_{q_3}^\beta\tau_{-q_1-q_2-q_3}^\beta+v\sigma_{q_1}^\alpha\tau_{q_2}^\alpha\sigma_{q_3}^\beta\tau_{-q_1-q_2-q_3}^\beta\} . \quad (39)$$

With the new parameters, v_1, v_2, and $\hat{w}$, we have seven recursion relations for the quartic terms, instead of just four, as using the previous form of the perturbation. A momentum-space Hamiltonian of this form has been mentioned, but not discussed, in the work of Mukamel and Grinstein.[7] With $v=0$, we regain a model Hamiltonian in a space of six parameters, which has been discussed by Fishman[8] and by Tamashiro and Salinas[10] in the context of a magnetic model with random anisotropies. In this particular case, at least in a calculation up to first order in ϵ, the fixed points describing the multicritical behavior are not stable. Moreover, there is an additional isotropic fixed point which cannot be reached from physically acceptable initial conditions.

Now it is not difficult to carry out a standard renormalization-group calculation to write the following recursion relations for the quartic terms:

$$u_1'=b^\epsilon\{u_1-4K_4[(8+n)u_1^2+6u_1v_1+\tfrac{1}{4}v^2-\tfrac{1}{2}vw+\tfrac{1}{4}nw^2+\tfrac{1}{2}w\hat{w}]\} , \quad (40)$$

$$v_1'=b^\epsilon\{v_1-4K_4[9v_1^2+12u_1v_1+\tfrac{1}{4}\hat{w}^2-\tfrac{1}{2}v\hat{w}]\} , \quad (41)$$

$$u_2'=b^{\epsilon}\{u_2-4K_4[(8+n)u_2^2+6u_2v_2+\tfrac{1}{4}v^2-\tfrac{1}{2}vw+\tfrac{1}{4}nw^2+\tfrac{1}{2}w\hat{w}]\}\ , \quad (42)$$

$$v_2'=b^{\epsilon}\{v_2-4K_4[9v_2^2+12u_2v_2+\tfrac{1}{4}\hat{w}^2-\tfrac{1}{2}v\hat{w}]\}\ , \quad (43)$$

$$w'=b^{\epsilon}\{w-4K_4[2w^2+(n+2)(u_1+u_2)w+3(v_1+v_2)w-v(u_1+u_2)+\hat{w}(u_1+u_2)+\tfrac{1}{2}v^2]\}\ , \quad (44)$$

$$\hat{w}'=b^{\epsilon}\{\hat{w}-4K_4[2\hat{w}(u_1+u_2)+3\hat{w}(v_1+v_2)+2\hat{w}^2+4w\hat{w}-3v\hat{w}-3v(v_1+v_2)]\}\ , \quad (45)$$

and

$$v'=b^{\epsilon}\{v-4K_4[2v(u_1+u_2)-v^2-\tfrac{1}{2}nv^2+4vw+v\hat{w}]\}\ , \quad (46)$$

where b is the rescaling factor and K_4 is a structure constant. For $n=0$, the set of fixed points with $v^*=0$ has been analyzed in great detail by Fishman and Aharony.[8] In this case, to order ϵ, there is a fully isotropic fixed point (in the space of n replicas) which is stable but cannot be reached from physically acceptable initial conditions. We then have a runaway of the flow lines, which is usually associated with the existence of a fluctuation-induced first-order transition. If we perform a higher-order calculation, there is also a stable decoupled fixed point, of order $\sqrt{\epsilon}$, which corresponds to a tetracritical point, with independent fluctuations of the two spin fields, and rules out the possibility of bicritical behavior. In the present case, however, the bare Hamiltonian already involves a term with $v>0$. An inspection of the recursion relations, with $n=0$, $u_1=u_2$, and $v_1=v_2$, indicates a runaway to a fixed point with $v^*\to+\infty$ (we can also have $v^*<0$, but this fixed point does not correspond to a physically acceptable situation). As in the case of the random-anisotropy models of Mukamel and Grinstein,[7] this runaway of the flow lines seems to suggest the occurrence of a fluctuation-induced first-order transition.

Let us consider the zero-replica limit of the recursion relations. First, we note that the coupling w is related to the fourth cumulant of the distribution $p(\eta_i)$. Therefore, we can analyze the case of a Gaussian distribution for which $w=0$. We also observe that the bare values of couplings u_1, u_2, and $\hat{w}$, vanish. These couplings are in fact generated by the renormalization-group flows, but they will be small with respect to the couplings v_1, v_2, and v, which are all positive in the bare Hamiltonian. We can now perform an analysis of the initial flow. For weak random couplings, the symmetry between the two systems is not broken. Hence, the physically accessible fixed points will be given by $u_1=u_2$, and $v_1=v_2$. Under these conditions, it is easy to see that $u_1=u_2$ and w will grow large and negative, and there will be no finite fixed value of v. Although rather strong, this is still a plausibility argument. Indeed, we note that the only term which may stop the v flow to large and positive values is given by the product $v\hat{w}$, where $\hat{w}>0$ is generated by the renormalization-group iterations. However, as the bare value of $\hat{w}$ vanishes, it is very unlikely that this term will be able to balance the effects of all the other terms which are driving v to large and positive values. This discussion also indicates that there may be a fixed point with $v<0$, which has no physical meaning and cannot be reached from initial values with $v>0$.

V. RELEVANCE OF THE RANDOM COUPLINGS

At this stage it is interesting to check the renormalization-group relevance of the random couplings. For very weak random interactions, $\langle\eta^2\rangle\ll 1$, the free energy is expected to behave as

$$g(\eta)=g(\eta=0)f\left[\frac{\langle\eta^2\rangle}{\Delta T^{\Phi}}\right]\ , \quad (47)$$

where Φ is the crossover exponent. The random perturbation is relevant, and the $\eta=0$ fixed point unstable, if $\Phi>0$. To calculate this crossover exponent, let us use a method outlined by Shapir and Aharony.[11] Keeping the most relevant terms, the replicated Hamiltonian may be written as

$$H^{(n)}=\sum_{\alpha=1}^{n}\left\{-J_1\sum_{(ij)}S_i^{\alpha}S_j^{\alpha}-J_2\sum_{(ij)}T_i^{\alpha}T_j^{\alpha}\right\}-\langle\eta^2\rangle\sum_{\alpha,\beta=1}^{n}\sum_{i=1}^{N}S_i^{\alpha}S_i^{\beta}T_i^{\alpha}T_i^{\beta}\ . \quad (48)$$

Taking the derivative of the free energy with respect to $\langle\eta^2\rangle$, we have

$$\frac{\partial g}{\partial\langle\eta^2\rangle}=\langle S_i^{\alpha}S_i^{\beta}T_i^{\alpha}T_i^{\beta}\rangle\ . \quad (49)$$

At $\eta=0$, the replicas are decoupled, and this derivative scales as $\langle S\rangle^2\langle T\rangle^2\sim\Delta T^{4\beta}$, where β is the critical exponent associated with the magnetization. From Eq. (47), at $\eta=0$, we also have

$$\frac{\partial g}{\partial\langle\eta^2\rangle}\sim g(\eta=0)\Delta T^{-\Phi}\sim\Delta T^{d\nu-\Phi}\ , \quad (50)$$

which yields

$$\Phi=d\nu-4\beta\ , \quad (51)$$

where ν is the critical exponent associated with the correlation length. Using a scaling relation, we can also write

$$\Phi=(4-d)\nu-4\eta\nu\ , \quad (52)$$

where η is the exponent associated with the decay of the critical correlations. Therefore, the random interactions are relevant for

$$4\eta<4-d\ , \quad (53)$$

which certainly holds for d just below four dimension. It also holds at $d=2$ and $d=3$. Then, $\Phi>0$ for $2\le d<4$, which confirms the relevance of the random couplings.

To complete this analysis, we now use the Imry-Ma argument to estimate the lower critical dimension for the stability of the mixed phase against fluctuations of the random couplings. Let us start with the mixed phase, with $m_1>0$ and $m_2>0$. We then reverse a domain of linear size L from $m_2>0$ into $m_2<0$. The gain in energy due to the fluctuations of concentration of random couplings $\pm\eta$ in the formation of the domain is of the order

$$E_r=\eta m_1 m_2 L^{d/2} \ . \tag{54}$$

At the same time, the formation of a domain wall costs the typical energy

$$E_w=2Jm_2L^{d-1} \ . \tag{55}$$

From these energy estimates, in the limit $L\to\infty$, and assuming that $m_1,m_2\neq 0$, we have $E_r>E_w$ for all $d<d_l=2$. Hence, in this range of dimension, the system breaks into domains and the mixed phase is unstable against weak random couplings. In other words, we say that an ordered component produces a random field of strength ηm which couples to the other component. On this basis, this problem is expected to have the same lower critical dimension $d_l=2$ as the random-field Ising model.

VI. CONCLUSIONS

We have performed detailed mean-field calculations for the phase diagram of a system of two Ising models with a random bilinear coupling. The successive transitions from a mixed to a simple ordered and finally to a disordered phase simulate the thermal behavior of a plastic crystal. Depending on the strength of the random couplings, the phase diagram displays different types of multicritical points. For a double-δ distribution, there is a tetracritical point which turns into bicritical as the strength of the couplings increases.

The phase diagram has been fully understood at the mean-field level. A momentum-space renormalization-group calculation was then performed to check the nature of the multicritical point. We resorted to the replica trick to write an effective n-component Hamiltonian up to quartic-order terms in the spin fields. Using the standard renormalization-group scheme, up to first order in $\epsilon=4-d$, we obtained a system of seven independent recursion relations to characterize the multicritical behavior. In the $n=0$ limit, we give some arguments to show that there is a runaway of the flow lines, which indicates the occurrence of a fluctuation-induced first-order phase transition.

The spin Hamiltonian introduced in this paper is simple enough to allow the performance of detailed calculations which provide an instrumental step towards the consideration of more realistic models. It may also be relevant to shed some light on the understanding of the behavior of plastic crystals.

ACKNOWLEDGMENTS

Y.S. acknowledges the donors of the Petroleum Research Fund, administered by the ACS, for the support of this research. He is also grateful for the hospitality of the Groupe de Physique des Solides at Université de Paris VI and VII, where parts of this work were done. S.G. and S.R.S. acknowledge grants from CNRS (France) and CNPQ (Brazil).

[1]K. H. Michel and J. Naudts, J. Chem. Phys. **67**, 547 (1987); K. H. Michel and J. M. Rowe, Phys. Rev. B **32**, 5818 (1985).

[2]J. A. Pople and F. E. Karasz, J. Phys. Chem. Solids **18**, 28 (1961); L. M. Amzel and L. N. Becka, J. Phys. Chem. Solids **30**, 521 (1969).

[3]S. Galam and M. Gabay, Europhys. Lett. **8**, 167 (1989).

[4]S. Galam, V. B. Henriques, and S. R. Salinas, Phys. Rev. B **42**, 6720 (1990).

[5]S. Galam, Phys. Lett. A **122**, 271 (1987); J. Appl. Phys. **63**, 3760 (1988).

[6]A. Aharony, Phys. Rev. B **12**, 1038 (1975).

[7]D. Mukamel and G. Grinstein, Phys. Rev. B **25**, 381 (1982).

[8]S. Fishman and A. Aharony, Phys. Rev. B **18**, 3507 (1978).

[9]J. Hubbard, Phys. Lett. A **39**, 365 (1972).

[10]M. N. Tamashiro and S. R. Salinas, Braz. J. Phys. **23**, 69 (1993).

[11]Y. Shapir and A. Aharoy, J. Phys. C **14**, L905 (1981).